



Bellcomm

955 L'Enfant Plaza North, S.W.
Washington, D. C. 20024

date: August 18, 1971

to: Distribution

B71 08023

from: G. M. Anderson, R. J. Ravera

subject: S-192 Multispectral Scanner
Performance Projections
Case 620

ABSTRACT

Performance projections for the S-192 Multispectral Scanner are presented based on recent detector parameter test data. These results are compared with Honeywell Radiation Center projections.

Some minor differences exist. Principally these are due to a more conservative treatment here of the effects of amplifier noise.


The results presented here show that for the channels analyzed, six are within the performance specification, two, or perhaps three, are slightly over the specification, and channel one is a factor of three over specification.

These projections represent a striking improvement over projections of the recent past due primarily to a remarkable improvement in detector properties.

(NASA-CR-121505) S-192 MULTISPECTRAL
SCANNER PERFORMANCE PROJECTIONS (Bellcomm,
Inc.) 20 p

N79-72517

00/19 Unclassified
12115

FF No. 6021	(PAGES)	(CODE)
	CR-121505	
	(NASA CR OR TMX OR AD NUMBER)	(CATEGORY)
		





Bellcomm

955 L'Enfant Plaza North, S.W.
Washington, D. C. 20024

date: August 18, 1971

to: Distribution

B71 08023

from: G. M. Anderson, R. J. Ravera

subject: S-192 Multispectral Scanner
Performance Projections
Case 620

MEMORANDUM FOR FILE

Introduction

This memorandum presents performance projections for the S-192 Multispectral Scanner based on current parameter test data* (see Ref. 1). The results are compared with Honeywell Research Center projections. Some minor differences exist principally due to the treatment of pre-amplifier noise.

Ref. 1 contains data on two detectors arrays:

51V - Number 1 flight array

79V - Developement array

Measurements of Noise Equivalent change in Reflectance ($NE\Delta\rho$) are presented for the 79V array. The detector - preamplifier time constant data are also presented. Normalized Detectivity, D^* , and bounds on tau detective, τ_d , are presented for the 51V array. These data are used to calculate $NE\Delta\rho$ performance for the 51V array.

There is a dramatic improvement in D^* values for the 51V array over the 79V array. These improvements range from a factor of 4.4 in channel 8 to a factor of 47.0 in channel 1.

Interest here is centered on the 51V array. The HRC data from Ref. 1 for this array are reproduced in Table 1. They show nine channels, 2-10, meeting the 1% $NE\Delta\rho$ specification, channel 1 being the only deviation.

An independent projection of $NE\Delta\rho$ is given here for the 51V array using a more conservative model for amplifier noise.

*Forwarded through the courtesy of Mr. W. E. Hensley, MSC.

CALCULATED NEAP VALUES FOR THE 51V NO. 1 FLIGHT ARRAY

Channel	A	D	D^*	τ_{pc}	τ_{dct}	Normalized Preamp Noise (Hz)	Normalized Detector Noise (Hz)	η_0	τ_a	H(λ)	NEAP ($^\circ$)
	Ad	CM Hz	$D^{1/2}$ /Watts	μ sec	μ sec	(Hz)	(Hz)	e		Watts/ CM ²	
1	3.2×10^{-4}	3.48×10^{44}		44	<1	6.88×10^4	1.92×10^5	0.0693	0.44	3.1×10^3	2.5
2	2.3	2.41		37		4.4×10^4		0.166	0.57	4.1	0.72
3	1.2	1.43		36		4×10^4		0.184	0.61	3.4	0.88
4	1.2	1.65		40		5.6×10^4		0.166	0.62	3.7	0.80
5	1.1	1.31		41		6×10^4		0.188	0.71	4.1	0.67
6	1.4	1.31		42		6.5×10^4		0.188	0.70	5.0	0.63
7	1.4	1.43		40		5.6×10^4		0.177	0.77	5.8	0.48
8	1.3	1.57		37		4.4×10^4		0.144	0.85	4.1	0.65
9	1.1	4.74		44		6.88×10^4		0.172	0.45	1.8	0.74
10	1.5	2.4		55		1.2×10^5		0.167	0.81	2.6	0.74
11			INDIVIDUALLY SELECTED					0.164			
12			"	"				0.154			

Table 1



Effects of Preamplifier Noise Bandwidth

Refs. 1 and 2 employ essentially identical expressions to compute $NE\Delta\rho$. For direct comparison we use Eq. (3.17) from Ref. 1:

$$NE\Delta\rho = \frac{4\sqrt{2A_d}}{H_{\Delta\lambda} \omega^2 D_0^2 D^*(0) \tau_a \tau_0} \left[\int_0^\infty \{ \hat{N}_d(f) + \hat{N}_p(f) \} |H_s(f)|^2 df \right]^{1/2} \quad (1)$$

where:

A_d = Area of the detector

D_0 = Effective diameter of the optical system

$D^*(0)$ = The low frequency detectivity of the system

$H_s(f)$ = The system transfer function

$H_{\Delta\lambda}$ = The solar irradiance in spectral band $\Delta\lambda$

$\hat{N}_d(f)$ = The detector noise Power Spectral Density (PSD)
normalized to the low frequency region of the
detector

$\hat{N}_p(f)$ = The preamplifier noise PSD normalized to the low
frequency region of the detector

ω = The instantaneous field of view

τ_a = The atmospheric transmission

τ_0 = The optical efficiency

The integral

$$\Delta f_n = \int_0^\infty \{ \hat{N}_d(f) + \hat{N}_p(f) \} |H_s(f)|^2 df \quad (2)$$



is basically the equivalent noise bandwidth of the system. The variable f is frequency (Hz). In Eq. (2),

$$\hat{N}_d(f) = \frac{1 + (f/f_d)^2}{1 + (f/f_{pc})^2} \quad (3)$$

where:

$$\begin{aligned} f_d &= 1/(2\pi\tau_d) \\ \tau_d &= \text{the detective time constant} \\ f_{pc} &= 1/(2\pi\tau_{pc}) \\ \tau_{pc} &= \text{the photoconductive time constant} \end{aligned}$$

From Eq. (3.6) of Ref. 1, HRC uses

$$\hat{N}_p(f) = 1.21 (\tau_d/\tau_{pc})^2 \quad (4)$$

The system transfer function, $H_s(f)$ is defined in Eqs. (3.7) through (3.14) in Ref. 1 and includes the preamplifier, 3RC poles, the boost network and the 2-pole Butterworth filter. The separate effects of $\hat{N}_d(f)$ and $\hat{N}_p(f)$ on the equivalent noise bandwidth as calculated by HRC are listed in columns 6 and 7 of Table 1 and are reproduced in Table 2. Results of the same computation repeated by the authors are listed in Table 2 for comparison. It is seen that agreement for the effect of detector noise is good while agreement for the effect of preamp noise is good only in channels 1 and 9. We were able to reproduce HRC's results for preamp noise by setting

$$\hat{N}_p(f) = 1.21(1/44)^2$$

for all channels. Clearly, however, Eq. (4) and column 4 of Table 1 indicate that the above value of $\hat{N}_p(f)$ is valid only for channels 1 and 9. Thus we do not agree with HRC's results for channels 2-8 and 10. The effect of this discrepancy on $NE\Delta p$ can be

EQUIVALENT NOISE BANDWIDTHS

CHANNEL	HRC			AUTHOR'S COMPUTATIONS		
	DETECTOR NOISE (HZx10 ⁻⁵)	PREAMP NOISE (HZx10 ⁻⁴)	TOTAL NOISE (HZx10 ⁻⁵)	DETECTOR NOISE (HZx10 ⁻⁵)	PREAMP NOISE (HZx10 ⁻⁴)	TOTAL NOISE (HZx10 ⁻⁵)
1	1.92	6.88	2.608	1.9166	6.882	2.6048
2	1.92	4.4	2.36	1.9166	6.885	2.6051
3	1.92	4.0	2.32	1.9166	6.886	2.6052
4	1.92	5.6	2.48	1.9166	6.884	2.6050
5	1.92	6.0	2.52	1.9166	6.883	2.6049
6	1.92	6.5	2.57	1.9166	6.883	2.6049
7	1.92	5.6	2.48	1.9166	6.884	2.6050
8	1.92	4.4	2.36	1.9166	6.885	2.6051
9	1.92	6.88	2.608	1.9166	6.882	2.6048
10	1.92	12.0	3.12	1.9166	6.879	2.6045

$$\hat{N}_p = 1.21 \left(\tau_d / \tau_{pc} \right)^2$$

TABLE 2



noted by comparing columns 2 and 3 of Table 3; the effect is admittedly small* if one accepts Eq. (4) as a correct representation of preamp noise PSD. If the multiplier in Eq. (4) is in fact larger than 1.21, the difference becomes more significant. Factors that influence this number are discussed next.

Preamplifier Normalized Noise PSD

There are three points to consider:

Noise Figure

HRC states that the noise figures of the 2N4405 transistors are 1.3 db for detector impedances in the 400-1000 Ω range. The Motorola data sheet, Figure 1, shows an optimum noise figure of 2 db for a source resistance of 80 Ω and a 1.0 mA bias. This means that the noise figure in the range 400-1000 Ω should be even greater than 2db and in fact should vary with detector resistance.

Differential Connection

The HRC analysis treats the preamp as single ended when in fact two transistors are operated as a differential pair.

Load Resistor

HRC does not take into account the effect of Johnson noise from the load resistor (2000 Ω at 300°K).

Taking these factors into account, we derive**

$$\hat{N}_p = 2.5989(\tau_d/\tau_{pc})^2, r_d = 240\Omega \quad (5)$$

$$\hat{N}_p = 3.7195(\tau_d/\tau_{pc})^2, r_d = 470\Omega \quad (6)$$

*Column 3 of Table 3 also includes other small numerical corrections and uses $\tau_a=0.47$ in channel 2 rather than $\tau_a=0.57$.

**See Appendix.

COMPARISON OF NE $\Delta\rho$ VALUES

<u>CHANNEL</u>	<u>HRC</u> <u>NE$\Delta\rho$ (%)</u>	<u>MODIFIED HRC</u> <u>NE$\Delta\rho$ (%)</u>	<u>NE$\Delta\rho$ (%)</u> <u>r_d = 240Ω</u>	<u>NE$\Delta\rho$ (%)</u> <u>r_d = 470Ω</u>
1	2.50	2.60	2.96	3.24
2	0.72	0.93	1.06	1.15
3	0.88	0.95	1.09	1.19
4	0.80	0.83	0.94	1.03
5	0.67	0.70	0.80	0.87
6	0.63	0.65	0.75	0.80
7	0.48	0.50	0.57	0.62
8	0.65	0.69	0.79	0.86
9	0.74	0.76	0.87	0.95
10	0.74	0.69	0.79	0.86

TABLE 3

PNP SILICON SWITCHING AND AMPLIFIER TRANSISTORS - 2N4405

SMALL-SIGNAL CHARACTERISTICS

NOISE FIGURE

$$V_{CE} = 10 \text{ Vdc}, T_A = 25^\circ\text{C}$$

FIGURE 9 - FREQUENCY EFFECTS

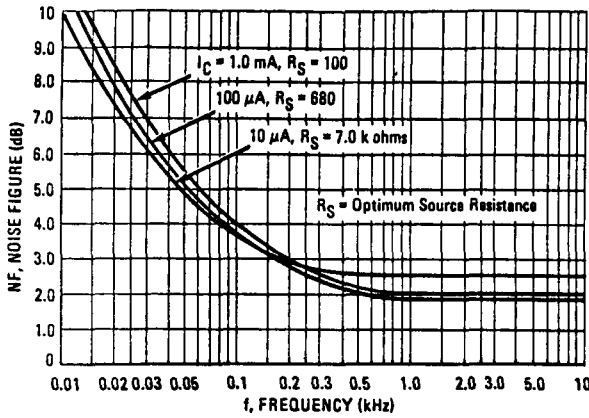
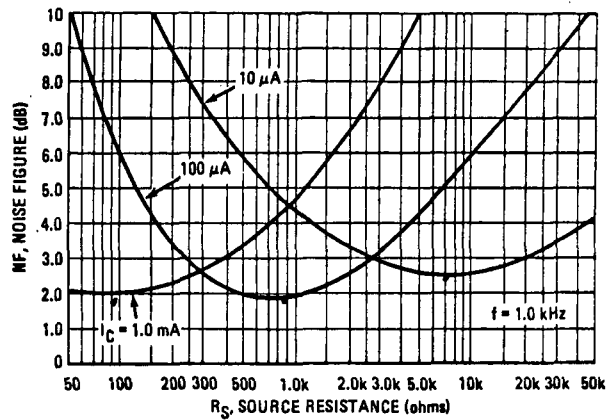


FIGURE 10 - SOURCE RESISTANCE EFFECTS



h PARAMETERS

$$V_{CE} = 10 \text{ Vdc}, f = 1.0 \text{ kHz}, T_A = 25^\circ\text{C}$$

This group of graphs illustrates the relationship of the "h" parameters for this series of transistors. To obtain these curves, 4 units were selected and identified by number - the same units were used to develop curves on each graph.

FIGURE 11 - CURRENT GAIN

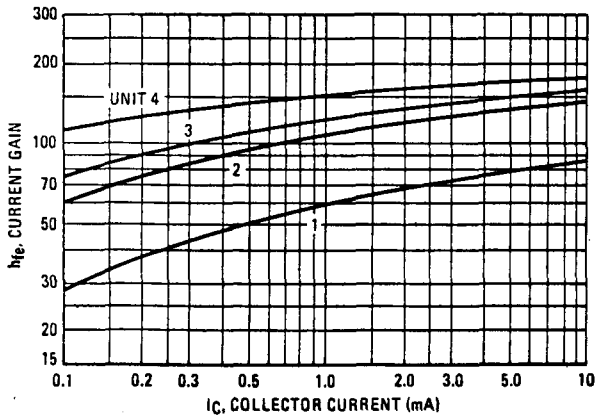


FIGURE 12 - INPUT IMPEDANCE

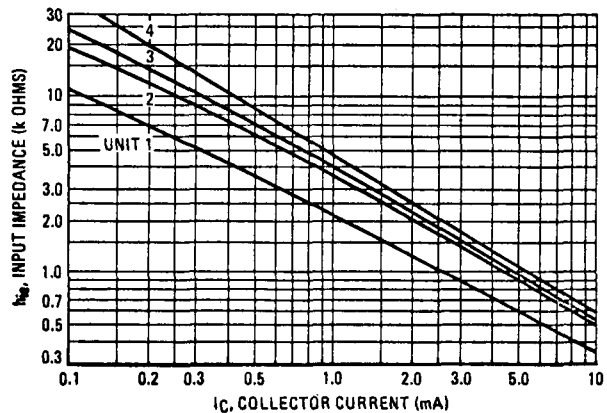


FIGURE 13 - VOLTAGE FEEDBACK RATIO

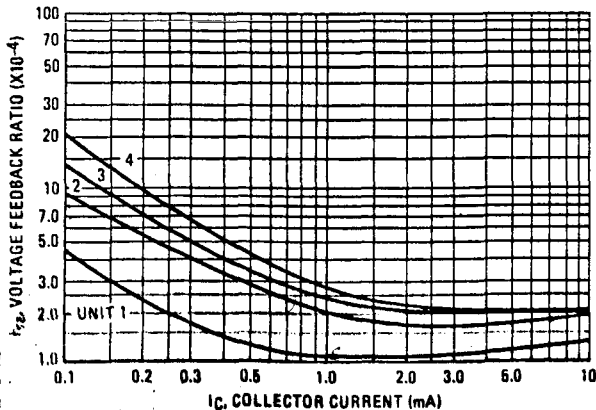
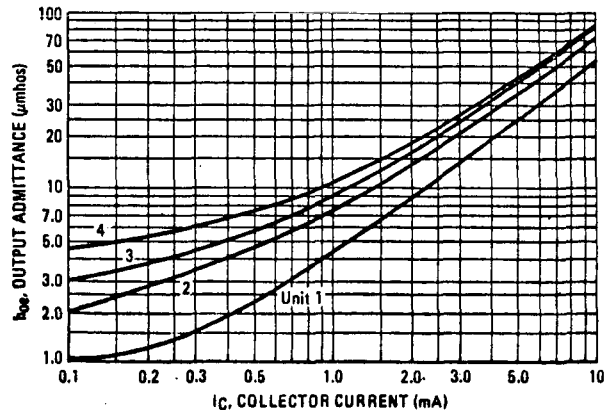


FIGURE 14 - OUTPUT ADMITTANCE



MOTOROLA INC. Semiconductor Products Division



where r_d is the detector resistance. Ref. 1 does not contain any data on detector resistances for the 51V array. We chose $240\Omega \leq r_d \leq 470\Omega$ based on the range of detector resistances found in the 79V array; they should serve as establishing representative bounds. Using Eqs. (5) and (6) along with Eqs. (1), (2) and (3), we computed a possible range of $NE\Delta\rho$ values; these are listed in columns 4 and 5 of Table 3. These results show that for the ten channels analyzed, six channels are within the 1% $NE\Delta\rho$ specification, two, or perhaps three, channels are slightly over the specification and channel one is a factor of three over specification.

HRC Experimental Results

We do not understand Figures 3 and 16 from Ref. 1, included in this memorandum. They show oscilloscope output used to experimentally determine $NE\Delta\rho$. Figure 3 is channel 1 for the 79V array while Figure 16 is channel 1 for the improved 51V array. We feel the outputs appear to indicate similar results and do not understand why Figure 3 yields a 20% $NE\Delta\rho$ while Figure 16 yields a 2% $NE\Delta\rho$.

Conclusions

Our calculations, based on HRC 51V detector array data of Ref. 1, indicate that the current HRC projections may be slightly optimistic. There is, however, a great improvement in performance over the 79V array due mainly to a dramatic improvement (ranging from a factor of 5 to a factor of 50) in values of D^* .

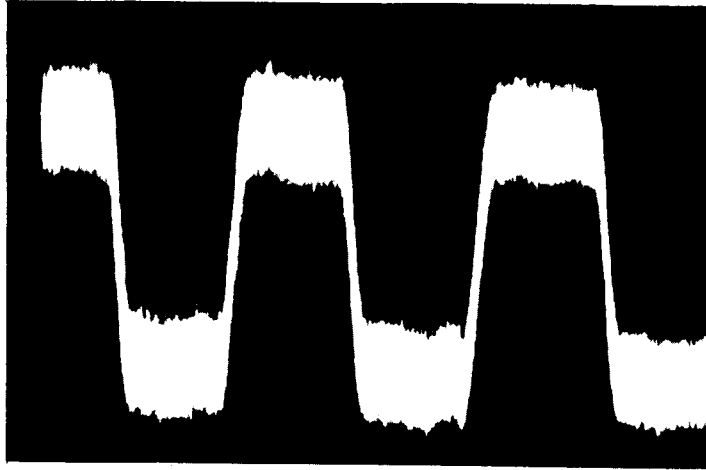

G. M. Anderson



1022-GMA-mef
RJR

R. J. Ravera

Attachments
Figures
Appendix
References



CHANNEL #1

79V Qual Array

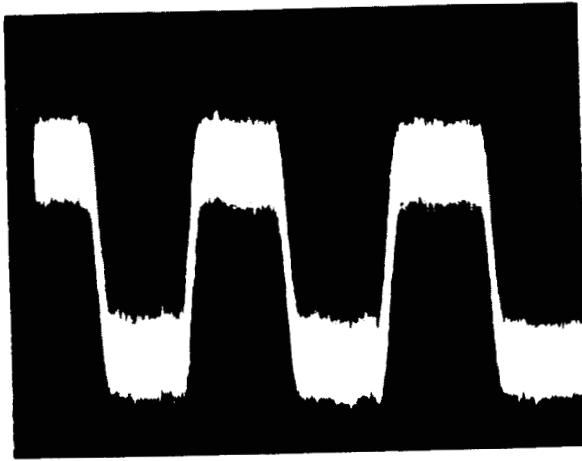
Radiometric Sensitivity
20% Reflecting Earth
 $NE\Delta\rho = 20\%$

V. SENS = 10MV/cm

H. SENS = 5msec/cm

NO RISE AND FALL TIME MEASUREMENTS

FIGURE 3



CHANNEL #1

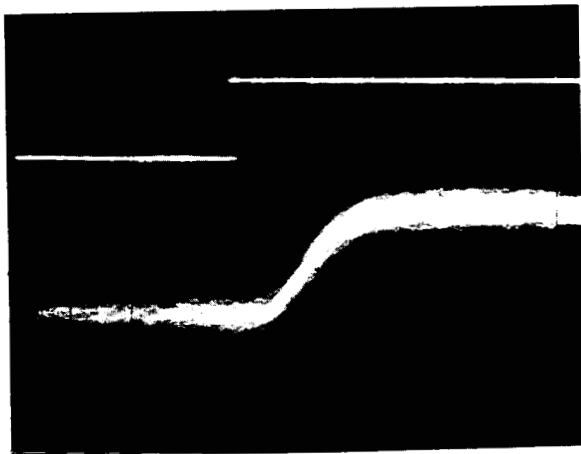
51V Array

Radiometric Sensitivity
20% Reflecting Earth

$NE\Delta\rho = 2\%$

V. SENS = 50MV/cm

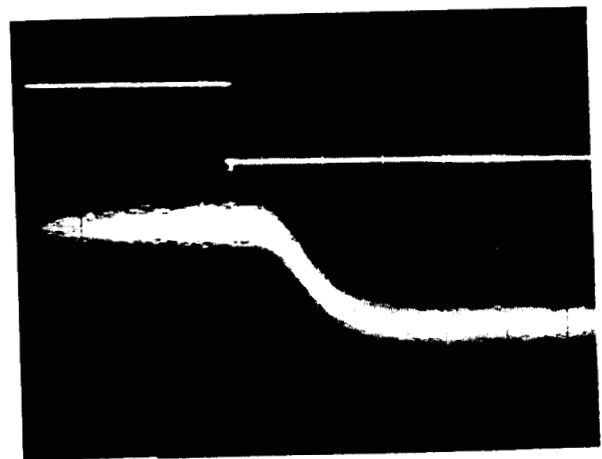
H. SENS = 20msec/cm



RISE TIME MEASUREMENT

H. SENS = $2\mu\text{ sec/cm}$

RISE TIME = $3.0\mu\text{ sec}$



FALL TIME MEASUREMENT

H. SENS = $2\mu\text{ sec/cm}$

FALL TIME = $3\mu\text{ sec}$

FIGURE 16



APPENDIX

We will outline in this section the method used to derive Eqs. (5) and (6), the normalized preamplifier noise Power Spectral Densities (PSD). It can be shown that the contributions of the Johnson noise PSD of the detector, the transistor noise PSD and the Johnson noise PSD of the detector load resistor to the preamplifier PSD are respectively given by*

$$N_{dj} = \frac{r_i}{(r_i + r_d)^2} 4kT_d r_d \quad (A-1)$$

$$N_T = \frac{\left(\frac{e_n}{\Delta f}\right)^2 r_i^2}{(r_i + r_d)^2} + \frac{\left(\frac{i_n}{\Delta f}\right)^2 r_d^2 r_i^2}{(r_i + r_d)^2} \quad (A-2)$$

and

$$N_L = \frac{r_i}{(r_L + r_i)^2} 4kTr_L \approx \frac{4kTr_i}{r_L} ; r_i \ll r_L \quad (A-3)$$

where $e_n/\sqrt{\Delta f} =$ equivalent noise voltage/Hz^{1/2} of differential preamplifier

$i_n/\sqrt{\Delta f} =$ equivalent noise current/Hz^{1/2} of differential preamplifier

$k =$ Boltzman's constant $= 1.38 \times 10^{-23}$ watt-sec-deg⁻¹

$r_d =$ detector resistance

$r_i =$ preamplifier input resistance

$r_L =$ detector load resistance

*We assume that $r_i \ll r_L$, $r_i \ll r_d$. The operational amplifier connection insures this condition.



T = temperature of the load resistor

T_d = temperature of the detector

Δf = bandwidth

The circuit diagram is reproduced in Figure A-1. Resistor r_L is r_5 and the reported value is $2k\Omega$. All the other resistors in the input circuit are capacitor bypassed. The total preamp noise PSD is obtained by summing (A-2) and (A-3):

$$N_p = N_T + N_L \quad (A-4)$$

It will be recalled from the definitions following Eq. (1) the preamplifier noise PSD normalized with respect to the detector low frequency noise PSD, $N_d(0)$, is required; that is $\hat{N}_p(f)$.

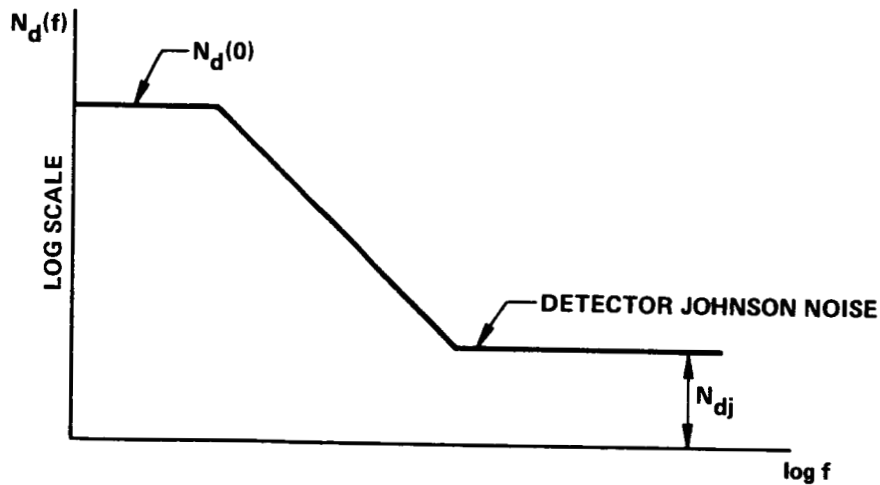
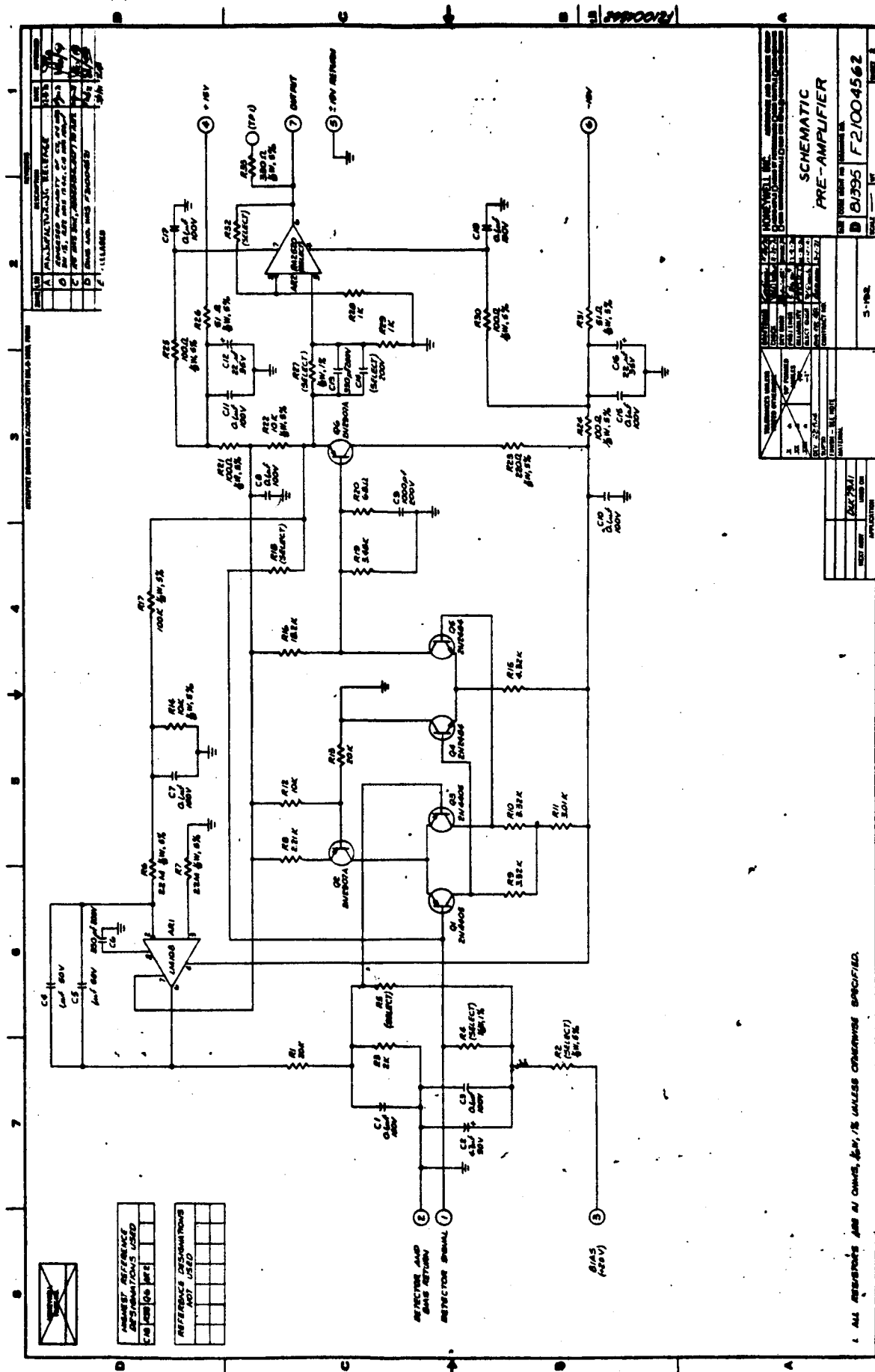


FIGURE A2 - DETECTOR NOISE PSD





The normalized detector noise PSD is given by

$$\hat{N}_d(f) = \frac{N_d(f)}{N_d(0)} \quad (A-5)$$

We may take the limit of (A-5) as f approaches infinity:

$$\lim_{f \rightarrow \infty} \hat{N}_d(f) = \frac{1}{N_d(0)} \lim_{f \rightarrow \infty} N_d(f) \quad (A-6)$$

From Eq. (3), it is clear that

$$\lim_{f \rightarrow \infty} \hat{N}_d(f) = \left(\frac{f_{pc}}{f_d} \right)^2 = \left(\frac{\tau_d}{\tau_{pc}} \right)^2 \quad (A-7)$$

From Figure A-2,

$$\lim_{f \rightarrow \infty} N_d(f) = N_{dj} \quad (A-8)$$

Combining (A-6), (A-7) and (A-8) and rearranging, we obtain the normalizing factor $N_d(0)$ in the form

$$N_d(0) = N_{dj} \left(\frac{\tau_{pc}}{\tau_d} \right)^2 \quad (A-9)$$

Dividing (A-4) by $N_d(0)$ yields

$$\hat{N}_p = \hat{N}_T + \hat{N}_L \quad (A-10)$$

where \hat{N}_T and \hat{N}_L can be obtained by dividing (A-2) and (A-3) by (A-9); thus,



$$\hat{N}_T = \frac{N_T}{N_d(0)} = \frac{N_T}{N_{dj} \left(\frac{\tau_{pc}}{\tau_d} \right)^2}$$

or from (A-1) and (A-2),

$$\hat{N}_T = \frac{1}{4KT_D} \left[\frac{\left(\frac{e_n}{\Delta f} \right)^2}{r_d} + \left(\frac{i_n}{\Delta f} \right)^2 r_d \right] \left(\frac{\tau_d}{\tau_{pc}} \right)^2 \quad (A-11)$$

Similarly, with the additional assumption that $r_i \ll r_d$, we can derive

$$\hat{N}_L = \frac{T}{T_D} \frac{r_d}{r_L} \left(\frac{\tau_d}{\tau_{pc}} \right)^2 \quad (A-12)$$

It remains to compute the quantities $\left(\frac{e_n}{\Delta f} \right)^2$ and $\left(\frac{i_n}{\Delta f} \right)^2$ in Eq. (A-11). The optimum noise figure for the transistors operated as a differential pair can be shown to be

$$F = 1 + \frac{2 \left(\frac{i_n}{\Delta f} \right)^2 (r_{d0})}{4KT} \quad (A-13)$$

where r_{d0} is the optimum source (detector) resistance and T is the temperature of the transistors. For the system under study, the Motorola 2N4405 transistor has the following characteristics:



$$F_{db} = 2$$

so that $F = 10^{F_{db}/10} = 10^{0.2} = 1.5849,$

$$r_{d0} = 160\Omega^*$$

and $T = 300^\circ K.$

Using these data, $(\frac{i_n^2}{\Delta f})$ may be computed from Eq. (A-13). The quantity $(e_n^2/\Delta f)$ is obtained from the fact that at the optimum noise figure,

$$e_n^2 = (r_{d0})^2 i_n^2 \quad (A-14)$$

In review, Eqs. (A-10), (A-11) and (A-12) can be combined to give

$$\hat{N}_p = \left\{ \frac{1}{4KT_D} \left[\frac{e_n^2}{r_d} + \left(\frac{i_n^2}{\Delta f} \right) r_d \right] + \frac{T}{T_D} \frac{r_d}{r_L} \right\} \left(\frac{\tau_d}{\tau_{pc}} \right)^2 \quad (A-15)$$

Based on values of $(\frac{e_n^2}{\Delta f})$ and $(\frac{i_n^2}{\Delta f})$ found from Eqs. (A-13) and (A-14) and on appropriate values of T , T_D , r_d and r_L , Eq. (A-15) was used to compute Eqs. (5) and (6) in the body of the memorandum.

*As used here r_{d0} is the optimum source resistance of the differential amplifier. As such it has a value twice that of the corresponding single ended value of 80Ω given in Figure 1.



References

1. "Radiometric Sensitivity Measurements and Calculations on S-192 Detector Arrays", A memo attached to Honeywell Radiation Center Customer Engineering Letter 71-CEL-130, June 25, 1971, R. A. Weagant and R. G. Blades.
2. "S-192 Multispectral Scanner Review", G. M. Anderson and R. J. Ravera, Bellcomm Memorandum for File B71 06007, June 4, 1971.



Subject: S-192 Multispectral Scanner
Performance Projections - Case 620

From: G. M. Anderson, R. J. Ravera

Distribution List

NASA Headquarters

H. Cohen/MLQ
J. H. Disher/MLD
J. P. Field, Jr./MLB
T. L. Fischetti/MLA
T. E. Hanes/MLA
A. S. Lyman/MR
M. Savage/MLE
W. C. Schneider/ML

MSC

C. E. Charlesworth/KA
W. E. Hensley/TD42
K. S. Kleinknecht/KA
T. R. Kloves/TD
C. L. Korb/TF
R. M. Machell/KW
O. G. Smith/KW
C. K. Williams/KS
J. G. Zarcaro/PD

Willow Run Laboratories

L. M. Larson

Bellcomm

A. P. Boysen
J. P. Downs
D. R. Hagner
W. G. Heffron
D. P. Ling
J. Z. Menard
J. M. Nervik
P. F. Sennewald
J. W. Timko
R. L. Wagner
M. P. Wilson
Departments 1011, 1013, 2031, 2034 Supervision
Departments 1022, 1024, 1025
Department 1024 File
Centtal File
Library